The Effects of Heat Treatment on the Grain Growth, Phase Evolution, and Hardness of Newly Developed Steel-based Hardfacing Alloys for Industrial Applications

Renee Kuzniar

California Polytechnic State University

Materials Engineering Senior Project

Advisor: Prof. Blair London

Corporate Sponsor: Scoperta Inc.

June 7, 2013

Approval Page

Project Title: The Effects of Heat Treatment on the Grain Growth, Phase Evolution, and Hardness of Newly Developed Steel-based Hardfacing Alloys for Industrial Applications

Author: Renee Kuzniar

Date Submitted: June 7, 2013

CAL POLY STATE UNIVERSITY

Materials Engineering Department

Since this project is a result of a class assignment, it has been graded and accepted as fulfillment of the course requirements. Acceptance does not imply technical accuracy or reliability. Any use of the information in this report, including numerical data, is done at the risk of the user. These risks may include catastrophic failure of the device or infringement of patent or copyright laws. The students, faculty, and staff of Cal Poly State University, San Luis Obispo cannot be held liable for any misuse of the project.

Prof. Blair London _____

Faculty Advisor Signature

Prof. Richard Savage _____

Department Chair Signature

Acknowledgements

I would like to thank my senior project sponsor Scoperta Inc. for providing funding as well as the samples to make my project possible. In particular John Madok, Justin Cheney, Dennis Zhang, and Jonathon Bracci from Scoperta provided me with the technical expertise on their complex Fe-based hardfacing alloys used for hardbanding. My advisor, Dr. Blair London, provided weekly deadlines and guidelines to support continued progress.

Abstract

Steel-based hardfacing alloys are welded onto the outside diameter of tool joints in three beads with a slight overlap between welds for underground drilling to prolong the tool joints' life. Current hardfacing alloys have a shortened life due to cracks occurring in neighboring weld beads. To decrease cracking, the effects of composition and heat treatment on the microstructure was investigated on five alloys. Five small arc-melt circular ingots roughly 1.4 x 0.3 inches were produced. Each sample had varying amounts of C, B, Cr, Mn, Mo, Nb, Si, Ti, V, and W. The carbon levels in the alloys were .91wt%, .98wt%, and 3 wt% resulting in a ferritic, martensitic, and austenitic matrix, respectively. The heat treated samples were solutionized at 1100°C for 2 hours, quenched followed by an aging treatment at 500°C for 5 hours and air cooled. Metallographic analysis was performed revealing the as cast microstructures to have a fine appearance compared to the coarser nature of the heat treated microstructures. Hardness values were measured and the effect of heat treatment on the ferritic and austenitic samples' hardness was minimal. Increasing the weight percent of Nb in the ferritic alloy prohibited grain growth resulting in slight changes in hardness after heat treatment, while increasing the weight percent of Ti had little effect. The martensitic sample decreased in hardness from 61 to 49 HRC due to the reduction in strain from heat treatment. Micro-hardness data revealed similar trends. Nano-hardness is suggested to understand microstructural evolution and measure ferrite hardness.

Keywords: Materials engineering, hardfacing, hardbanding, solutionize, steel

Table of Contents

List of Figures

List of Tables

Introduction

Problem Statement

Hardfacing alloys are commonly deposited on the outside diameter of tool joints for underground drilling to increase wear resistance, in a process known as *hardbanding*. The joint is pre-heated to 500°F; three beads of Scoperta's steel-based hardfacing alloy are then sequentially welded onto the joint with a slight overlap between welds. Upon weld depositing the alloys Scoperta currently uses, there is susceptibility to cracking in neighboring weld beads. The goal of this project is to understand microstructural changes in the hardbanding as a function of heat treatment to minimize cracking and increase wear resistance of the deposited coatings.

What is Hardbanding?

Hardbanding is a process where a hardfacing material is welded onto tool joints for underground drilling to protect from abrasive wear (Figure 1). The hardfacing material is typically applied using gas metal arc welding. Hardbanding has been used in industry since the late 1930s and increases a tool joint's wear life[1]. The most extensive wear on underground drilling is found on tool joints rather than drill pipes due to a larger diameter of the tool joint compared to the drill pipe tubing. Tension, compression, and rotation are factors causing wear on the tool joint, which is in constant contact with either the open hole or the casing wall[1]. Hardbanding's ultimate goal is to increase the service life of tool joints.

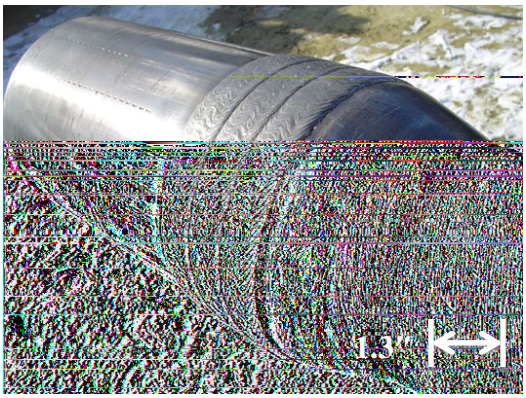

Figure 1: Tool joint for underground drilling showing three hardfacing beads, known as hardbanding, sequentially welded[2].

Prior to more sophisticated drill techniques used such as deep well and horizontal drilling, using Tungsten Carbide (WC) hardbanding adequately protected tool joints. Due to the limited use of casing while drilling, casing wear was not of great concern. As the demand for underground oil drilling increased, WC particles started breaking off during service causing increased wear instead of protecting the tool joints. WC particles broken off act as an abrasive agent, which is more destructive than the earth's siliceous nature, due to WC's higher hardness. WC is also an expensive mechanism to use for hardbanding[3].

In 1990, new hardbanding materials were introduced into the drilling industry to meet the increased demands on tool joints from higher multidirectional forces experienced in drilling highly deviated wells such as horizontal and extended reach drilling[4]. These higher forces increased drag and torque on tool joints. Therefore, hardfacing materials need to continue to adapt to meet the increasingly complex forces from grinding and grounding abrasion[4].

Project Justification

When hardbanding is deposited onto the outside diameter of tool joints, two to four beads of steel-based hardfacing alloys are sequentially gas metal arc deposited with a slight overlap between each weld pass. Newly developed alloys have been prone to develop micro-cracks during their application due to their complex microstructural nature[3]. As a result of cracking, premature failures and spalling occur resulting in a need for reapplication[3]. Each bead is sequentially welded to reduce application time, labor cost, and energy. A common issue during application is cracking in neighboring weld beads reducing the abrasive wear resistance of the hardfacing (Figure 2).

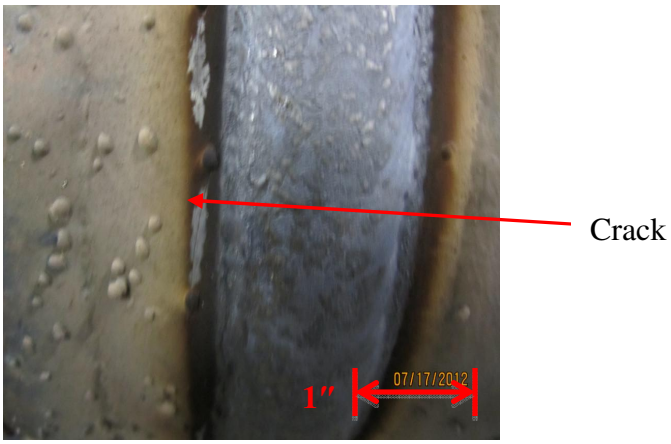

Figure 2: Cracking occurring between weld beads during processing[5].

During welding, different phase evolution occurs which is thought to cause cracking. Understanding the phase evolution as a function of temperature during application is critical to understanding why cracking is occurring. Often the grain size in the under weld is larger than the grain size in the over weld due to the under weld's longer exposure to heat (Figure 3).

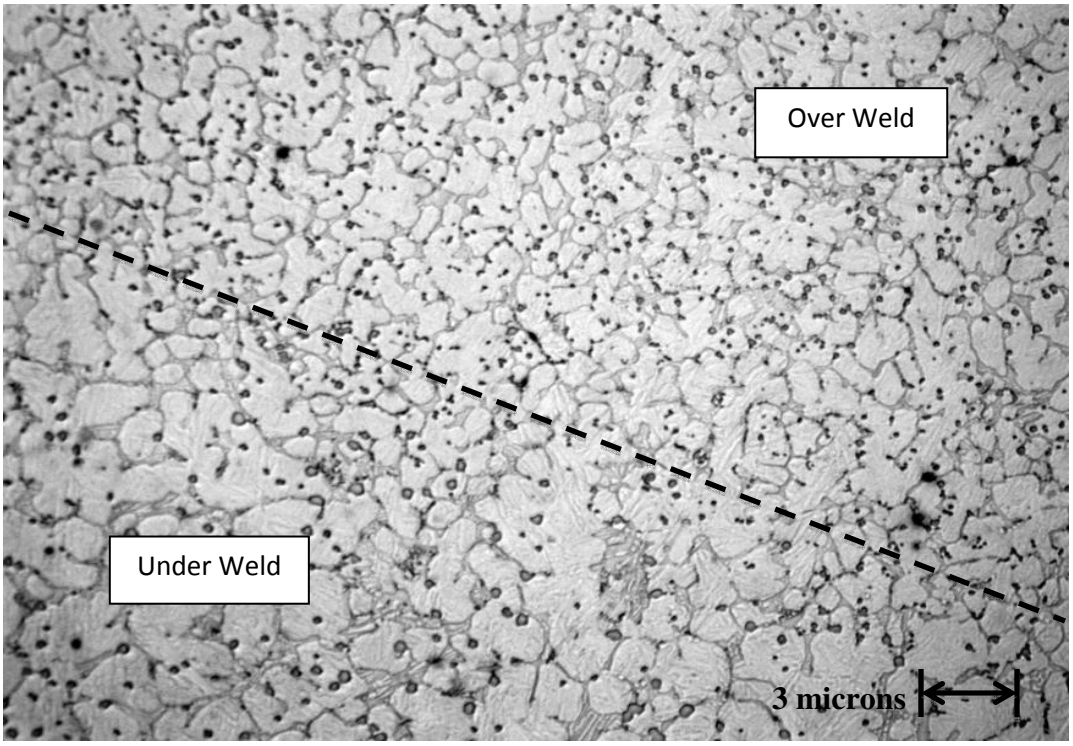

Figure 3: The under weld experienced grain growth while the over weld was deposited due to longer exposer to heat[5].

Steel-Based Hardfacing Alloys for Hardbanding

Steel-based hardfacing alloys have been found to be the optimal hardfacing materials. A hardfacing alloy must have a high hardness, 50-65 HRC, which is achieved through carbides formed from alloying elements in steel. Siliceous earth particles have a hardness of about 64 HRC; therefore, in order to withstand abrasion carbides must have a comparable hardness[6]. Primary carbides have a hardness of around 125-155 HRC but their ferritic matrix's hardness is around 32-57 HRC depending on the carbon content in the ferrite[6].

Due to carbides' brittle nature, they are notch sensitive, which causes localized stresses, or stress risers leading to cracking. To reduce notch sensitivity, carbides are distributed in a tough ferritic matrix to help transfer the load and reduce crack propagation[6]. The best hardfacing alloy used for hardbanding should have a fine microstructure as the carbides produce wear

resistance while the ferritic matrix transfers the load to the carbides. Alloying elements currently used to produce these carbides are categorized into three categories (Table I).

Table I: Alloying Elements Functionality in Microstructures for Hardfacing Materials[7]

Function	**Alloys**
Austenite Phase Stabilizers	C, Mn, Ni
Ferrite Phase Stabilizers	Cr, Si, Mo, Al
Carbide Forming Elements	Cr, Nb, W, V, Mo

Chromium, Niobium, Vanadium, Tungsten, and Molybdenum have high affinities for carbon, an indication of strong carbide formers. Chromium Carbide is the first to precipitate from the liquid phase for hardfacing alloys with a hypereutectic composition[8]. Due to Chromium Carbides' precipitation from the liquid phase, they are uniformly distributed throughout the structure, which is desirable to reduce stress concentrations. The stoichiometric composition of the precipitated carbides is Cr_7C_3 with a prismatic crystal structure and has a hardness of about 125 HRC[8]. Molybdenum, Niobium, Titanium, and Vanadium form secondary carbides, which precipitate and are embedded throughout the eutectic matrix improving wear resistance[8].

Common crystal structures of carbides found in steel based hardfacing alloys are summarized in Table II. Often carbides and their morphologies are dependent on the processing technique used and the alloy composition of the particular hardfacing alloy. The crystal structures summarized are thermodynamically calculated and differing carbide morphologies may be found due to kinetically favorable reactions. Carbides containing higher coherency with the ferritic body centered cubic (BCC) matrix also may lead to less stress on the microstructure reducing cracking.

Table II: Carbides Formed in High Alloy Steels and Their Corresponding Crystal Structure and Lattice Parameter[8]

Carbide	Structure	Lattice Parameters (nm)		
		a	*b*	*c*
Cr				
$M_{23}C_6$	FCC	1.06228		
$Cr_{23}C_6$	**FCC**	**1.06599**		
$(Cr,Fe)_7C_3$	**Hexagonal**	**1.398**		**0.4523**
Cr_7C_3	**Hexagonal**	**1.398**		**0.4523**
Cr_7C_3	**Orthorhombic**	**0.70149**	**1.2153**	**0.4532**
Cr_3C_2	**Orthorhombic**	**0.55273**	**1.14883**	**0.28286**
Fe				
Fe_3C	**Orthorhombic**	**0.50915**	**0.67446**	**0.45276**
Fe_3C	**Orthorhombic**	**0.5091**	**0.67434**	**0.4526**
Fe_7C_3	Hexagonal	0.6882		0.454
Fe_2C	Hexagonal	0.2754		0.4349
Fe_2C	Orthorhombic	0.4704	0.4318	0.283
Mo				
$(MoFe_2)C$	Orthorhombic	1.627	1.003	1.132
Mo_2C	FCC	0.4155		
Mo_2C	Orthorhombic	0.4732	0.6037	0.5204
Mo_2C	Hexagonal	0.301204		0.47352
Mo_2C	Hexagonal	4.8259		0.9468
MoC	Hexagonal	0.2932		1.097
MoC	Hexagonal	0.2901		0.2786
Nb				
NbC	**FCC**	**0.44698**		
V				
VC	**Cubic**	**0.833409**		
W				
WC	**Hexagonal**	**0.29062**		**0.28378**
W_2C	Hexagonal	0.2997		0.47279
$(W_4Ni_2)C$	FCC	1.125		
$(W_3Fe_3)C$	FCC	1.11094		

Carbides with a FCC and HCP crystal structure such as NbC and Fe_7C_3 are semi-coherent with ferrite's BCC crystal structure. If chromium is present in the alloy, the thermodynamically stable carbide is Cr_7C_3; however, often $Cr_{23}C_6$ carbides are also present from non-equilibrium solidification during the cooling rate of conventional processing. In other words their formation

is kinetically driven[8]. Due to the precipitation of Cr_7C_3 from the liquid phase, these carbides act as a nucleation site for $Cr_{23}C_6$ as chromium diffusion occurs.

Vanadium is often used in hardfacing alloys and also precipitates from the liquid phase as Vanadium Carbide with a 1:1 stoichiometry. Vanadium Carbides contain a high negative free energy change acting as a large driving force in comparison to chromium and molybdenum[8].

Boron is also a common alloy used in steel-based hardfacing alloys due to its ability to form a fine microstructure and the inherent hardness of boron carbides. Boron concentrations of 1-1.5 wt % have been experimentally found to reduce grain size in Fe-based hardfacing alloys (Figure 4)[9].

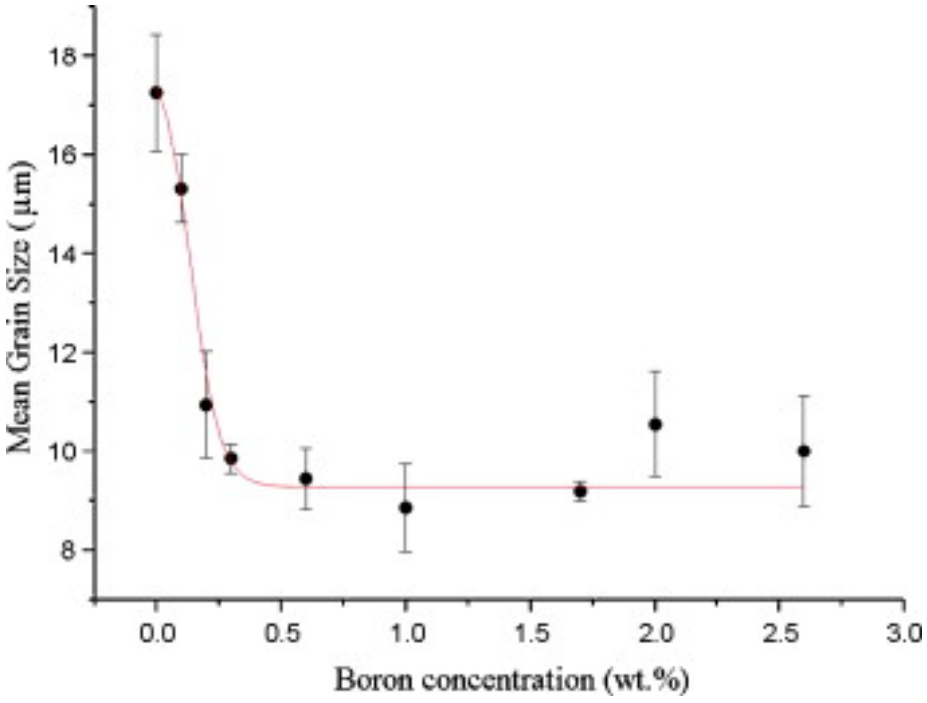

Figure 4: Mean grain size versus boron concentration in an Fe-based hardfacing alloy, showing concentration from 1-1.5 wt% B have the smallest mean grain size[9].

A reduction in the mean grain size strengthens the matrix leading to an increase in abrasive wear resistance. At concentrations of 1-1.5 wt% B results in the formation of primary borides such as Cr_2B and TiB_2[5].

Phase Evolution During Heat Treatment

Due to primary carbides' low tensile strength during application they tend to pull apart from the matrix during cooling after arc-melt welding and in neighboring welds[10]. Therefore, when applied by arc-melt welding shrinkage cracks may form across weld beads[10]. It is critical the application of hardfacing alloys must be applied crack free by minimizing the phase evolution of primary carbides and the matrix during pre-heat and post-cooling[10]. Nucleation and grain growth is undesirable during arc-melt welding of the under weld during hardbanding application at elevated temperatures of around 400-600°C[5]. Strain is also created from primary carbides' low tensile strength between weld beads when the under weld ferritic region experiences grain growth.

Current Hardfacing Testing

Due to the ever changing demands of underground oil drilling, a lack of hardbanding material guidelines exists in industry[10]. New tests involve finding the coefficient of thermal expansion (CTE) of the weld overlay to the base metal, which is typically 4137 modified steel. In order to reduce cracking between the base material and the hardfacing alloy, the misfit strain is measured. However, the CTE is not linear with temperature change. The difference in misfit strain is calculated as a function of temperature for alloys under consideration and compared to 4137 modified steel using the equation:

$$\varepsilon = \Delta\alpha * \Delta T \quad (1)$$

where ε is the misfit strain, $\Delta\alpha$ is the coefficient of thermal expansion, and ΔT is the temperature difference. The misfit strain is used for temperatures from 100°C to 700°C with a reference temperature of 25°C in order to further understand what is occurring in the heat affected zone[10].

Constitutional Liquation

Constitutional liquation often occurs during welding and causes cracking in the heat affected zone (HAZ). The theory comes from the discovery of solute-rich liquid pools between two differing solid phases forming below the solidus temperature of an alloy[11]. Although hardfacing alloys have a more complex phase diagram than a eutectic binary system, a simplified version of constitutional liquation will be explained (Figure 5). When alloy X_1 is heated to T_1 the phase diagram states that a solid with an α-matrix and A_xB_y precipitates will be present. However, due to rapid heating between welds in the HAZ, when the temperature reaches T_E and eventually $T_{solidus}$ there is not enough time for diffusion and the alloy cannot reach thermodynamic equilibrium. Since thermodynamic equilibrium cannot be reached the A_xB_y precipitates will not fully dissolve changing the composition of the alloy due to solute rich liquid pools, which start to form around precipitates[12]. When cooling back to $T_{solidus}$ after the 2nd welded band of hardfacing is applied, the B rich liquid is unstable and does not solidify at the same rate as α-phase grains forming. Once the temperature drops further the B rich liquid around the α-grains is unable to diffuse due to rapid cooling. Once the B rich liquid with a higher melting point cools and expands, stress is created on the α-matrix causing cracking[12].

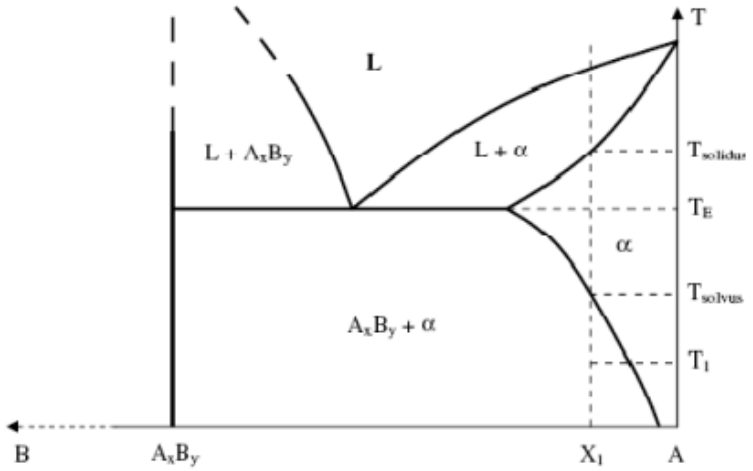

Figure 5: A binary phase diagram with A_xB_y precipitates as the cause of constitutional liquation. For the given explanation of constitutional liquation alloy X_1 is considered[12].

Broader Impacts to Improve Hard-facing Alloys for Hardbanding

The United States consumed 6.87 billion barrels of oil in 2011 and 7 billion barrels of refined petroleum products and bio-fuels in 2010, which is 22% of the world petroleum consumption[13]. Due to the large amount of petroleum and oil consumption, it is critical that hardfacing alloys decrease a tool joints abrasion wear and increase its maximum service life.

For the past 60 years hardbanding problems have cost millions of dollars in repairs and sometimes lead to well abandonment. Drill string repair and replacement is equally expensive. Not only is the replacement expensive, the cost of paying laborers and lost rig time to changing out worn down components is a costly process for drilling companies[4].

The cost of replacing failed hardbanding and tooling includes: previous hardbanding removal, mild steel build up, re-application of the hardbanding, and mild steel machining (Figure 6). A need for easy re-application, robust adhesion, and longevity must be achieved to reduce replacement costs companies face[3].

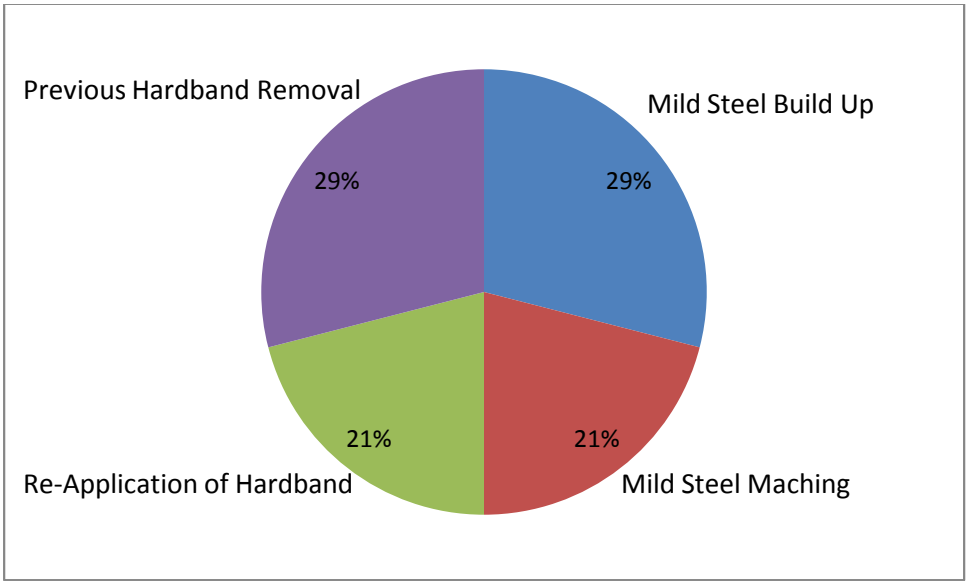

Figure 6: Relative cost of replacing each component when substantial tool joint abrasion occurs due to hardbanding failure at tool joints for underground drilling[3].

Realistic Constraints

Manufacturability

Scoperta's process of applying their current hardfacing alloy in three bands by arc welding could not be performed for each newly developed alloy because Scoperta does not manufacture the tool joint itself. Since cracking is occurring between the first and second hardband weld, analysis of the newly developed hardfacing alloys deposited on the tool joints would have been best to understand why cracking is occurring. To utilize fast paced testing techniques with lab sized alloys, heat treatments were performed on smaller size ingots to simulate welding parameters.

Health and Safety

2% Nital etchant used to reveal microstructures was prepared under a fume hood to reduce exposure to nitric acid. Rubber gloves, goggles, and a safety apron were used when preparing and etching samples under the fume hood. The nitric acid and etchant were disposed of in the proper acid waste container.

Procedure

Sample Preparation

Rapid development software was used by Scoperta to evaluate millions of potential alloys (Figure 7). Alloys were selected based on the lowest melting temperature determined by Scoperta's software. The lower the melting temperature, the closer the alloy is to the eutectic composition. The closer an alloy is to the eutectic composition the finer the microstructure resulting in a high hardness. Five alloy compositions were chosen as candidates to lower cracking based on the criteria above.

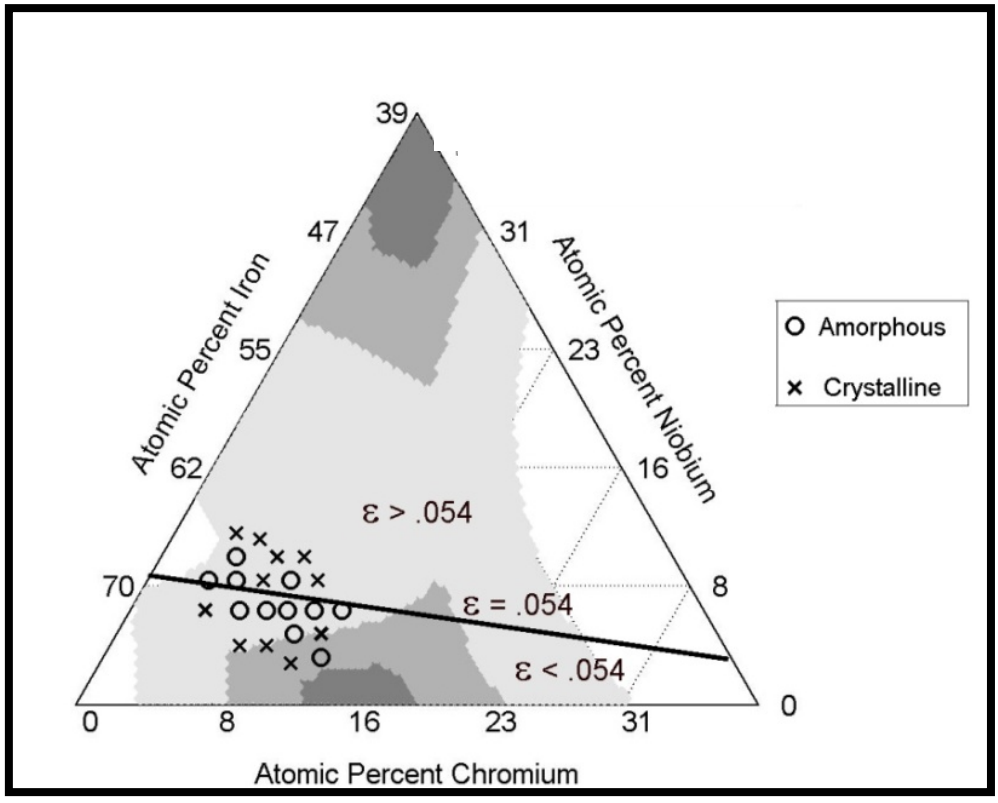

Figure 7: Quaternary Fe-Nb-Cr phase diagram with the lowest melting temperature alloys in dark gray. The alloys in the dark gray region are closest to the eutectic composition. Alloys shown intersecting the line were considered as hardfacing alloys[5].

Once the alloys were selected, Scoperta personnel arc-melted 1.3″ X 0.3″ cylindrical ingots. The five different alloy compositions were achieved by weighing each elemental component into a crucible and melting them together in a vacuum melter. Two samples of each alloy were made. Alloy 1, 350XT, is Scoperta's current hardfacing alloy solution for

hardbanding (Table III). Alloy 2, 350XT (Ti), contains the same composition as 350 XT with a .61 wt% increase of Ti. While Alloy 3, 350XT (Nb), contained the same composition as 350XT with a 1.46 wt% increase of Nb. Austenitic Alloy 4, AHB-35, had the highest amount of carbon at 3 wt%. Martensitic Alloy 5, 161XT, contained the second highest carbon at .98 wt %.

Table III: Fe-based Hardfacing Alloys Selected Using Scoperta's Rapid Development Software[5]

Alloy	Class	W	B	C	Cr	Mn	Mo	Nb	Si	Ti	V	Fe
350XT	**Ferritic**	**0**	**1.45**	**.91**	**4.82**	**1.01**	**3.22**	**4.54**	**.59**	**.39**	**.54**	**bal.**
350XT (Ti)	**Ferritic**	**0**	**1.45**	**.91**	**4.82**	**1.01**	**3.22**	**4.54**	**.59**	**1**	**.54**	**bal.**
350XT (Nb)	**Ferritic**	**0**	**1.45**	**.91**	**4.82**	**1.01**	**3.22**	**6**	**.59**	**.39**	**.54**	**bal.**
AHB-35	**Austenitic**	**5**	**0**	**3**	**5**	**10**	**0**	**4**	**0**	**.2**	**.5**	**bal.**
161XT	**Martensitic**	**0**	**1.2**	**.98**	**2.25**	**1**	**0**	**1**	**.4**	**.25**	**.5**	**bal.**

One ingot of each alloy was solutionized at 1100°C for 2 hours and water quenched in order to redistribute all of the alloying elements. The samples were then aged at 500°C for 5 hours and air-cooled, allowing numerous complex intermetallic carbides to precipitate. A diamond saw with a CBN Metal Bonded Wafering Blade was used to section roughly equal .2″ portions of the heat treated and as cast alloys for microstructural analysis and hardness measurements.

Macro-Hardness

Ten sectioned alloys, five heat treated and five as cast, were macro-hardness tested using a Wilson Rockwell Hardness Tester on the HRC scale. The alloys were tested in seven random locations and an average of each test was recorded.

Optical Microscopy

After hardness data was collected, the as cast and heat treated alloys were mounted in mineral filled Diallyl Phthalite Bakelite. Standard metallographic procedures were used to polish each sample. The samples were etched with 2% Nital to differentiate between phases. An optical microscope was used to analyze microstructures and capture metallographic images at 500x and 1000x.

Mirco-Hardness

The alloys were micro-hardness tested while mounted at a load of 500gf using a Micromet 2100 Series Micro-Hardness Tester. The alloys were tested in seven random locations and the values were reported along with an average of all tests performed. The values were measured in Vickers and converted to HRC to compare the macro and micro-hardness values.

X-Ray Diffraction

An X-Ray Diffraction (XRD) scan was performed on the hardbanding 350XT alloy where cracking was occuring. The X-rays were taken using a Cu-Kα source. A scan increment of .04 degrees with a scan speed of eight seconds per increment was used. The scanning range was 10°-100° and the scan time was 5 hours.

Results

Macro-Hardness Analysis

The average macro-hardness of 350XT, 350XT (Ti), AHB-35, and 161XT decreased after heat treatment while 350XT (Nb) had the same macro-hardness after heat treatment (Figure 8). The martensitic alloy, 161XT, had the most variation in hardness, decreasing by 12 HRC.

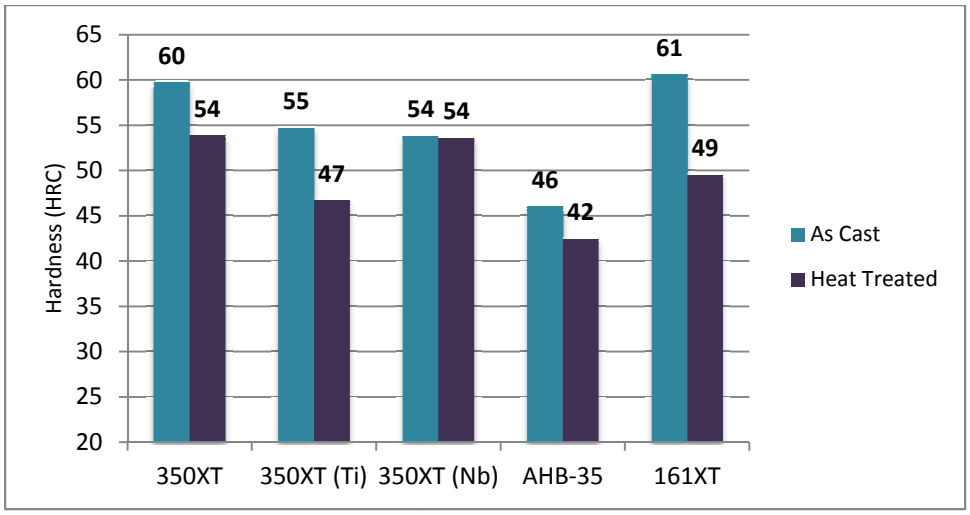

Figure 8: Macro-hardness values in HRC for the as cast and heat treated alloys.

Micro-Hardness Analysis

The average micro-hardness of each alloy had similar trends as macro-hardness data (Figure 9). AHB-35 showed the same as cast and heat treated average micro-hardness. In general, micro-hardness values were greater than the macro-hardness, as the smaller indenter for micro-hardness is more affected by carbide particles than the larger indenter used for macro-hardness. Macro-hardness produces an averaging effect because of the larger indenter. 350XT had the largest decrease in micro-hardness after heat treatment followed by 161XT. 350XT (Ti) and AHB-35 had the same as cast and heat treated micro-hardness.

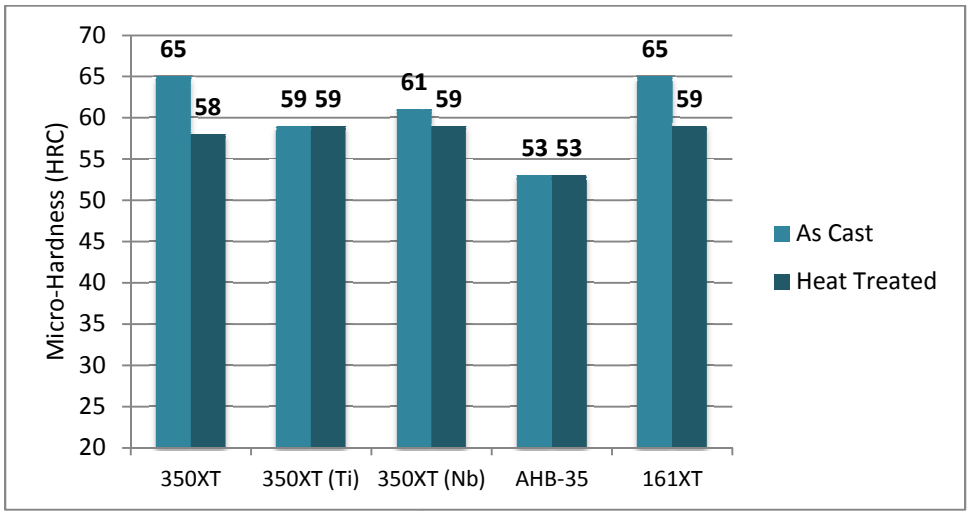

Figure 9: Micro-hardness values converted to HRC for the as cast and heat treated alloys.

Microstructural Results

Microstructural evolution was investigated by metallographic analysis from the as cast and heat treated alloys. Ferritic alloy 1, 350XT, showed significant grain growth after being solutionized and aged (Figure 10). The lighter phase in the as cast and darker phase in the heat treated microstructure is ferrite. The darker and lighter phase in the as cast and heat treated microstructures, respectively is a phosphorus-chrome-boron eutectic. The grain growth in the heat treated microstructure reflected in a decrease in both micro and macro-hardness values. The darker grains in the heat treated alloy had a lower micro-hardness.

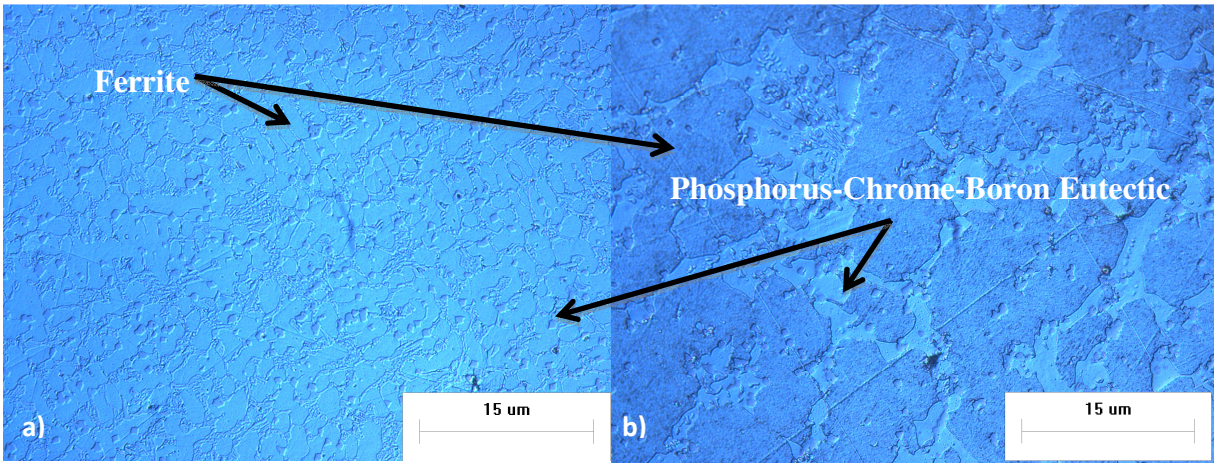

Figure 10: a) As cast and b) heat treated microstructures of ferritic alloy 350XT, Scoperta's current hardfacing alloy solution at 500x etched with 2% Nital.

A similar trend of grain growth was observed in 350XT (Ti) when compared to Scoperta's current 350XT hardfacing alloy (Figure 11). The as cast appearance of 350XT (Ti) was finer than Scoperta's current hardfacing alloy, 350XT. A more homogeneously distributed matrix with precipitates was observed from heat treatment. The lighter region of the as cast microstructure is ferrite and the darker region is a phosphorus-chrome-boron eutectic and vice versa for the heat treated microstructure (Figure 11).

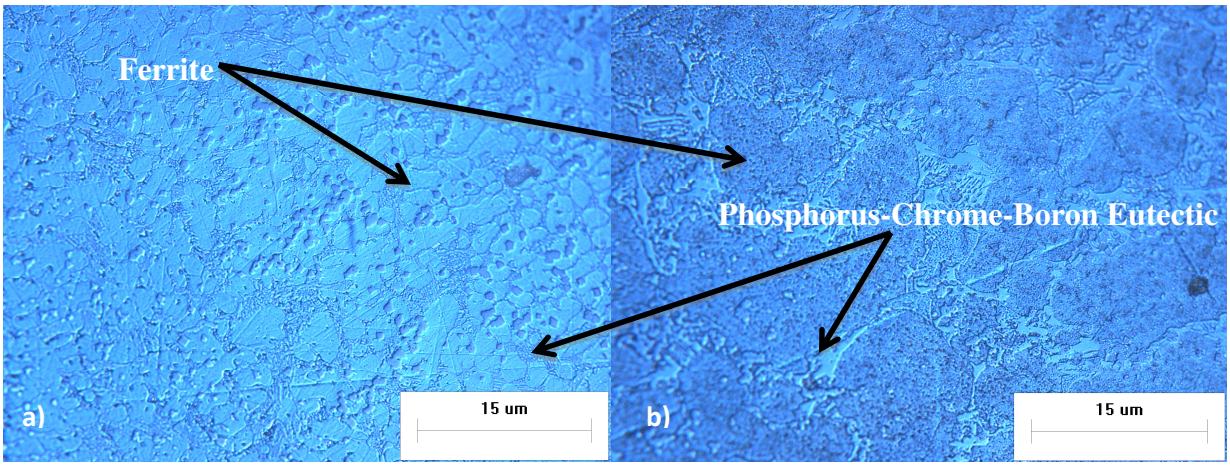

Figure 11: a) As cast and b) heat treated microstructures of ferritic alloy 350XT (Ti) at 500x etched with 2% Nital.

The as cast microstructure of ferritic Alloy 3, 350XT (Nb) had the finest microstructures of the three ferritic alloys (Figure 12). Grain growth occurred from the aging heat treatment; however, the grain growth was smaller when compared to 350XT, and 350XT (Ti). The fine appearance of both the as cast and heat treated alloy correlated with minimal changes in micro and macro-hardness values.

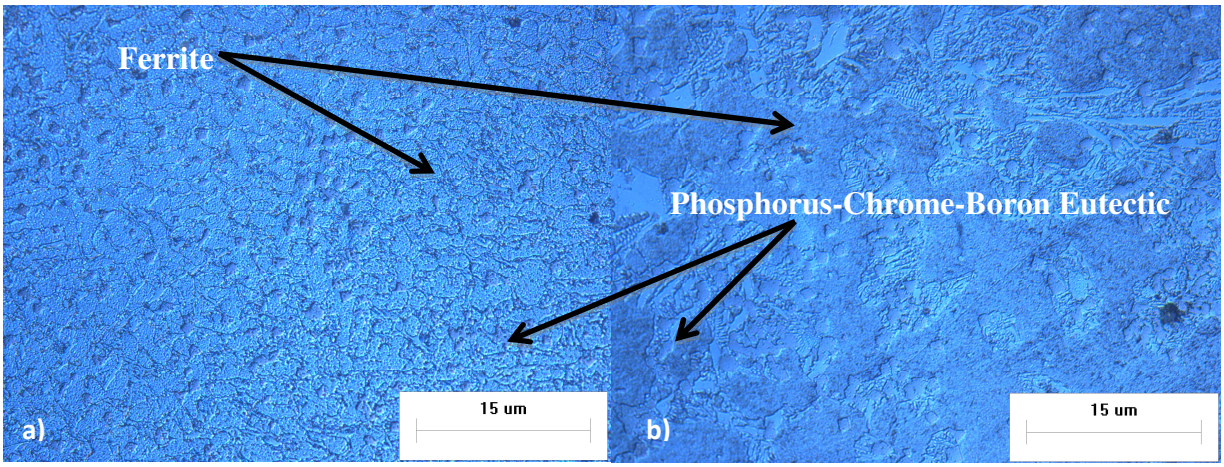

Figure 12: a) As cast and b) heat treated microstructures of ferritic alloy 350XT (Nb) at 500x etched with 2% Nital.

Large austenitic dendrites were observed in the as cast microstructure of the austenitic alloy, AHB-35 (Figure 13). After heat treatment, needle like structures were observed in the center of the alloy. The raised portion of the microstructure is the eutectic composition.

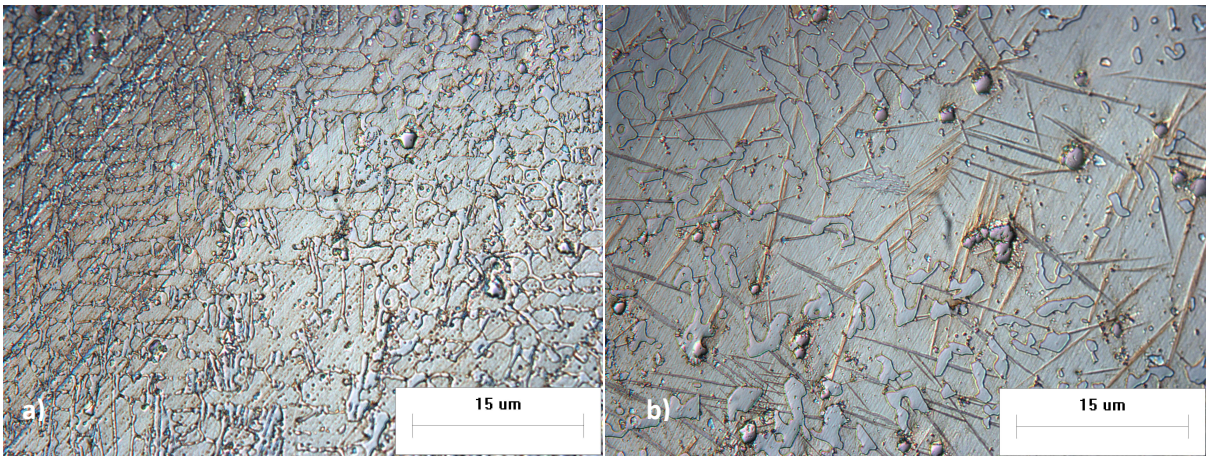

Figure 13: a) As cast and b) heat treated microstructures of austenitic alloy AHB-35 at 500x etched with 2% Nital.

The martensitic alloy, 161XT, had the finest as cast appearance due to the high strain in as cast martensite. Because of 161XT's martensitic nature there was a lack of distinctive grains in the as cast microstructure. A significant amount of diffusion occurred after heat treatment and a much coarser microstructure with larger grains resulted (Figure 14). When micro-hardness testing the darker grains in the heat treated alloy had a lower hardness value.

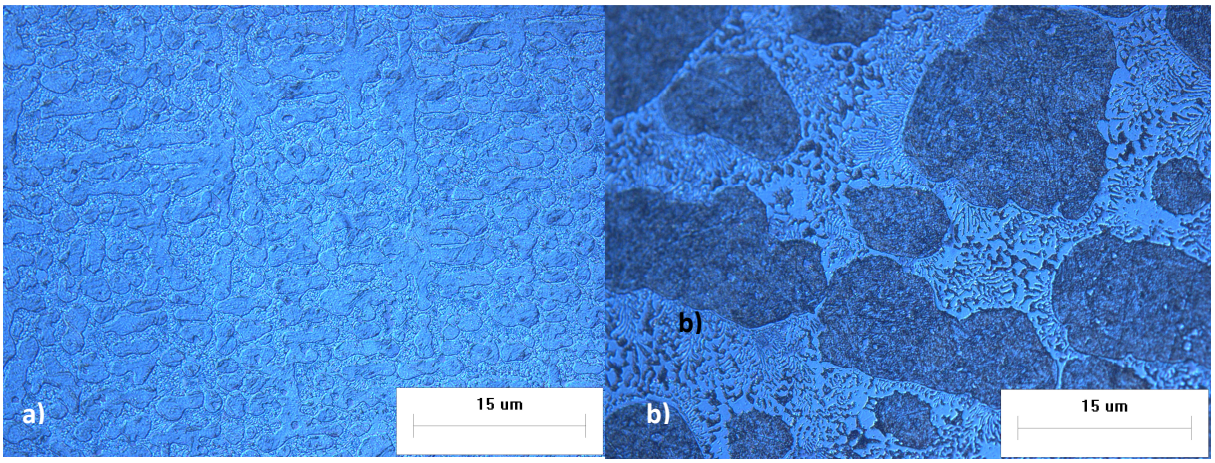

Figure 14: a) As cast and b) heat treated microstructure of martensitic alloy 161 XT at 500x etched with 2% Nital.

X-Ray Diffraction Results

XRD results did no reveal any intermetallic carbides due to the complex microstructure of 350XT. The broad peak revealed that amorphous phases exist within the microstructure (Figure 15). A BCC ferritic phase matched the first major peak from the XRD scan (Figure 15). However, due to database limitations, lacking the complex intermetallic carbides in 350XT, a definitive identification of the crystallographic structure of the carbides and phases was not possible.

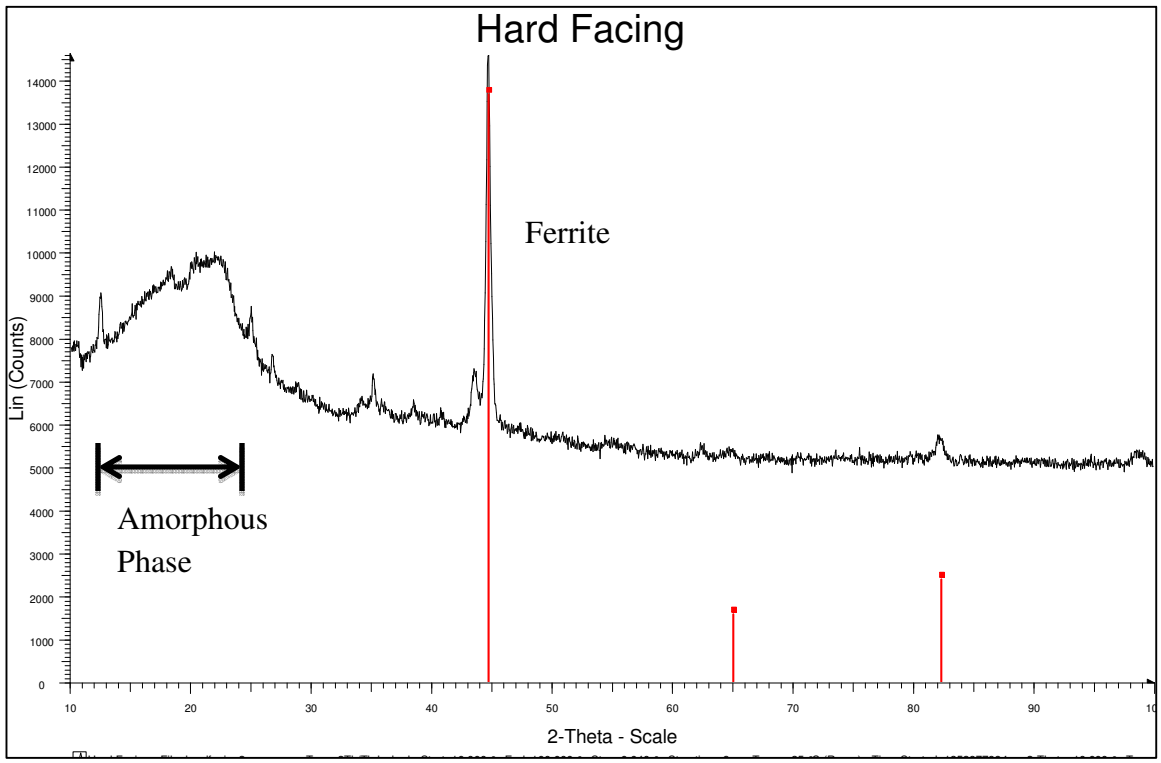

Figure 15: XRD scan of 350XT taken from the hardbanding on a tool joint.

Although many of the peaks from the XRD scan did line up with intermetallic carbides in the database, the matches were not distinctive enough to confirm intermetallic carbides such as NbC, FeC, and CrC existed.

Discussion

Hardness

According to World Oil a typical hardness for an adequate hardfacing alloy used for hardbanding is 50-60 HRC[7]. Therefore, AHB-34 would not have a high enough hardness in both the as cast and heat treated conditions due to its macro-hardness of 46 and 42 HRC, respectively. 350XT (Ti) also decreased in macro-hardness below typical hardfacing values after heat treatment from 55 to 47 HRC, respectively. The amount of carbon in the ferrite matrix in the case of 350XT, 350XT (Ti), and 350XT(Nb) has a large influence on the hardness. Carbon increases the hardness of the matrix due to interstitial solid solution strengthening. Although AHB-35 had the highest amount of carbon at 3 wt%, due to austenite's FCC crystal structure there are more slip planes for plastic deformation to occur resulting in a lower hardness than the other alloys.

Since the amount of Ti and Nb increased by .61 and 1.46 wt % in the 350XT (Ti) and 350XT (Nb), respectively it is thought they are forming intermetallic carbides lowering carbon's wt% in the ferritic matrix. To test the theory of decreased carbon in the ferritic matrix resulting in a lower hardness due to carbide formation it was desired to perform nano-indentation on the ferritic matrix. Due to the high cost of a Berkovech tip used for nano-indentation, and time constraints the nano-hardness could not be tested. However, future testing is recommended to determine if the ferritic matrix of 350XT, 350XT (Ti), and 350XT (Nb) is maintaining hardness after heat treatment using a nano-indentor.

Minimal grain growth observed in 350XT (Nb) from heat treatment correlated with little changes in both macro and micro-hardness. NbC's have low solubility in austenite, the lowest of all refractory metal carbides. Micrometer size NbC precipitates are virtually insoluble in steels at all processing temperatures and are located on grain boundaries[14]. NbC precipitates prevented excessive grain growth in 350XT (Nb) due to its 1.46 wt% increase of Nb compared to the 350XT and 350XT (Ti) resulting in little changes in hardness.

Microstructural Evolution

The phase evolution thermodynamically expected in 350XT was calculated by Scoperta (Figure 16). The solidification sequence is read as temperature decreases from right to left with decreasing mole fraction of each phase. In the case of the phase evolution shown for 350XT, liquid is first to form followed by NbC, TiB_2, ferrite, Cr_2B, and finally (Cr,Fe)C. Since (Cr,Fe)C forms at the lowest temperature it may transform in the heat affected zone where ferrite converts to austenite creating a different thermal expansion coefficient leading to cracking[5].

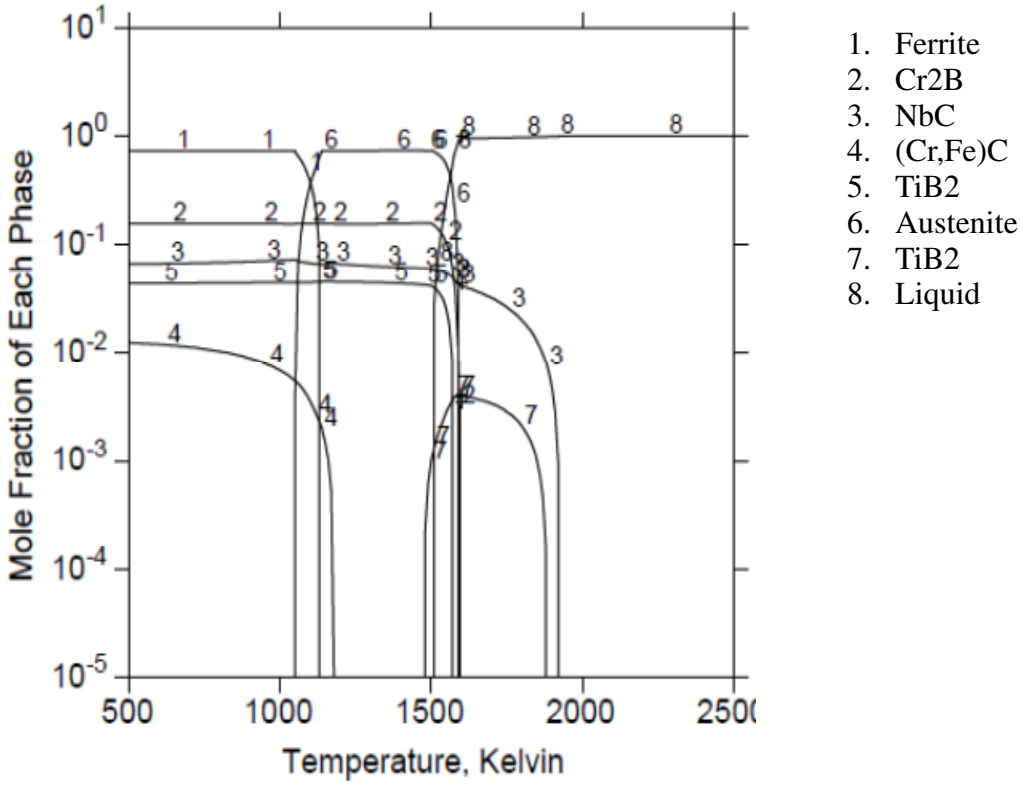

Figure 16: Thermodynamically expected phase evolution of 350XT showing the phase relationship read from right to left as temperature decreases and a decreasing mole fraction of each phase.

A darker region was observed outlining grain boundaries and the phosphorus-chrome-boron eutectic phase in between welds from a tool joint containing Scoperta's current hardbanding alloy, 350XT (Figure 17). Darker outlines around grain boundaries and solute-rich phases are an indication this portion was last to solidify. The formation of solute-rich liquid pools from constitutional liquation may be occurring in the HAZ causing cracking between the 1st and 2nd weld.

In particular, incoherent precipitates such as TiB_2 are known to have subsolidus liquation due to kinetically driven reactions[15]. NbC precipitates are also incoherent in a BCC ferritic matrix; however, dissolution of Nb rich precipitates raises the local liquidus temperature of the alloy[15]. Therefore, constitutional liquation is not as common when NbC intermetallic precipitates are present[15].

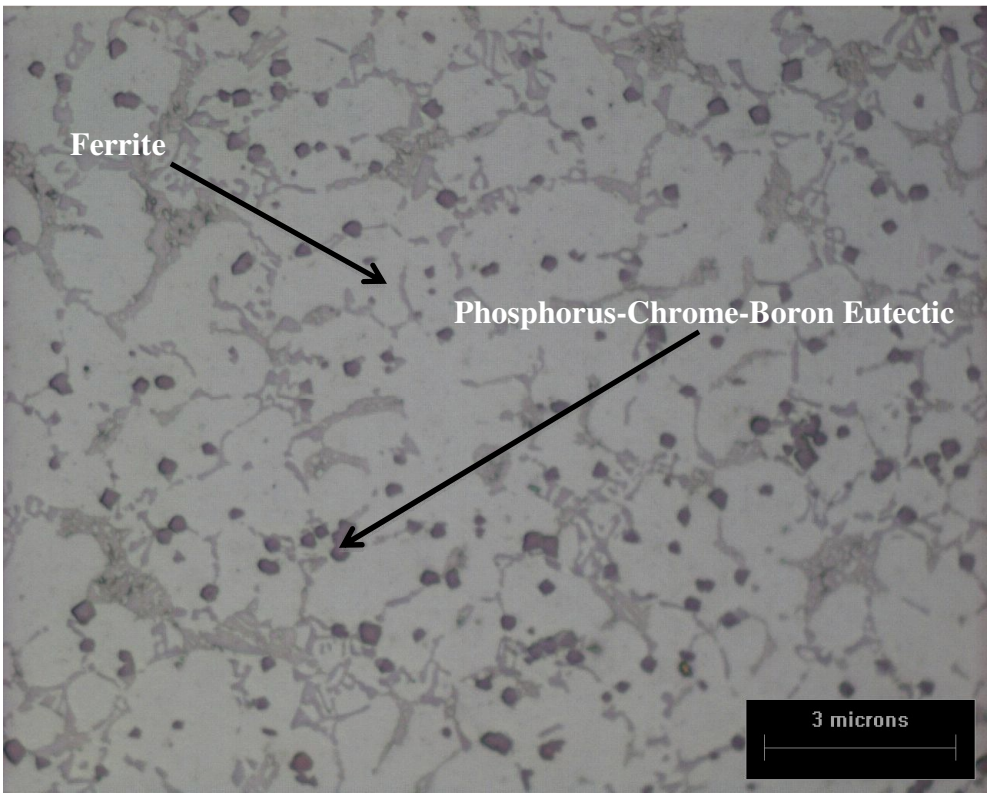

Figure 17: 350XT microstructure from hardbanding on a tool joint etched with 2% Nital.

Heat-treating the five possible Fe-based hardfacing alloy solutions to simulate welding parameters did not have the same extreme variance in temperature experienced in neighboring welds. Therefore, to determine if solute-rich pools are forming at grain boundaries in the heat affected zone, Gleeble testing is recommended. Due to the ingot size constraint, 1.4″ X 0.3″, of Scoperta's developed alloys this was outside the scope of the project.

Recommendations

It is recommended that Scoperta welds cylindrical ingot rods 5″ long and .25″ in diameter. Gleeble testing uses resistance heating to simulate the rapid heating in the HAZ of a neighboring weld. In particular an Anneal Strength Gleeble test should be generated. The Anneal Gleeble Strength test would determine at what temperature the HAZ of an alloy is pulling apart at a nominal force of 20lb[11]. This is achieved by determining the nil strength temperature, nil ductility temperature, and ductility to recover temperature revealing the brittle temperature range and crack susceptibility region[11]. The larger the temperature difference to pulls apart the alloy from the alloy's melting point the more likely constitutional liquation is occurring.

Conclusions

1. The as welded and heat treated alloys had minimal changes in hardness.
2. Cracking in between welds is not due to embrittlement of the entire microstructure as the macro and micro-hardness did not increase from heat treatment.
3. The smallest grain growth and microstructural changes was observed in 350XT (Nb) due to the low solubility of NbC carbides in austenite.

References

1. Murthy, G., Goutam, D., Swapan, D., Nikhat, P. "Hardbanding Failure in a Heavy Weight Drill Pipe." *Materials Science and Technology.* Volume 18, Issue 5, Pages 1395-1402.
2. "Iron Based Hardfacing 1/16 in 1.6mm Stoody HB-5633." *Victor Technologies.*
3. Miller, B. "Hardbanding Technology Advances." Duraband NC Certified for Re-Applications. *Postle Industries Inc.*
4. Mobley, J. "Hardbanding and its Role in Directional/Horizontal Drilling." *Society of Petroleum Engineers.* Pages 28-31.
5. Cheney, Zhang. "Scoperta Overview." *Scoperta Inc.*
6. Daemen, R. (2002). "Hardfacing Alloy, Methods, and Products." United States Patent: US 6375895 B1
7. Mobley, J., Daemen, R. "A Metallurgical Approach to the Design of Hardbanding Alloys. Arnco Technology.*" World Oil.* ATT Technology Ltd.
8. Hetzner, D., and William V. "Crystallography and Metallography of Carbides in High Alloy Steels." *Materials Characterization* 59 (2008): 825-41. Print.
9. Kim, Ji, Kang Ko, Gyung Kim, and Seung Noh. "The Effect of Boron on the Abrasive Wear Behavior of Austenitic Fe-based Hardfacing Alloys." *Wear* 267.9-10 (2009): 1415-419. Print.
10. Chan, A., Hannahs, D., Jellison, M., Breitsameter, M., Branagon, D., Stone, H., Jeffers G. (2008). "Hardband Technology Gets Tougher." *World Oil.* Vol 229 No. 7.
11. Ojo, O., & Tancret, F. (2008). Clarification on ''Thermo-Calc and Dictra Simulation of Constitutional Liquation of Gamma Prime (γ') During Welding of Ni-Base Super Alloys". Computational Materials Science.
12. Savage, W., & Page, J. (1967). "Effects of Constitutional Liquation in 18Ni Maraging Steel Weldment." Welding Journal, 12, 411.
13. US Energy Information Administration. *US Petroleum Consumption Data and World Oil Consumption*.
14. "Niobium Carbide." *Wikipedia*. Wikimedia Foundation, 26 Apr. 2013.
15. Radhakrishnan. "Interface Controlled Precipitate Dissolution and Constitutional

Liquation." Department of Materials Science and Engineering University of Alabama at Birmingham. *Interface Science, 1, 175-182 (1993).*